# Motoneuronal and muscle synergies involved in cat hindlimb control during fictive and real locomotion: a comparison study

**Sergey N. Markin, Michel A. Lemay, Boris I. Prilutsky and Ilya A. Rybak**

*J Neurophysiol* 107:2057-2071, 2012. First published 21 December 2011; doi:10.1152/jn.00865.2011

*J Neurophysiol* 107: 2057–2071, 2012.
First published December 21, 2011; doi:10.1152/jn.00865.2011.

# Motoneuronal and muscle synergies involved in cat hindlimb control during fictive and real locomotion: a comparison study

**Sergey N. Markin,[1] Michel A. Lemay,[1] Boris I. Prilutsky,[2] and Ilya A. Rybak[1]**
[1]*Department of Neurobiology and Anatomy, Drexel University College of Medicine, Philadelphia, Pennsylvania; and* [2]*Center for Human Movement Studies, School of Applied Physiology, Georgia Institute of Technology, Atlanta, Georgia*

Submitted 22 September 2011; accepted in final form 20 December 2011

**Markin SN, Lemay MA, Prilutsky BI, Rybak IA.** Motoneuronal and muscle synergies involved in cat hindlimb control during fictive and real locomotion: a comparison study. *J Neurophysiol* 107: 2057–2071, 2012. First published December 21, 2011; doi:10.1152/jn.00865.2011.—We compared the activity profiles and synergies of spinal motoneurons recorded during fictive locomotion evoked in immobilized decerebrate cat preparations by midbrain stimulation to the activity profiles and synergies of the corresponding hindlimb muscles obtained during forward level walking in cats. The fictive locomotion data were collected in the Spinal Cord Research Centre, University of Manitoba, and provided by Dr. David McCrea; the real locomotion data were obtained in the laboratories of M. A. Lemay and B. I. Prilutsky. Scatterplot representation and minimum spanning tree clustering algorithm were used to identify the possible motoneuronal and muscle synergies operating during both fictive and real locomotion. We found a close similarity between the activity profiles and synergies of motoneurons innervating one-joint muscles during fictive locomotion and the profiles and synergies of the corresponding muscles during real locomotion. However, the activity patterns of proximal nerves controlling two-joint muscles, such as posterior biceps and semitendinosus (PBSt) and rectus femoris (RF), were not uniform in fictive locomotion preparations and differed from the activity profiles of the corresponding two-joint muscles recorded during forward level walking. Moreover, the activity profiles of these nerves and the corresponding muscles were unique and could not be included in the synergies identified in fictive and real locomotion. We suggest that afferent feedback is involved in the regulation of locomotion via motoneuronal synergies controlled by the spinal central pattern generator (CPG) but may also directly affect the activity of motoneuronal pools serving two-joint muscles (e.g., PBSt and RF). These findings provide important insights into the organization of the spinal CPG in mammals, the motoneuronal and muscle synergies engaged during locomotion, and their afferent control.

spinal cord; motoneurons; walking; one-joint muscles; two-joint muscles; cluster analysis

THERE IS ACCUMULATING EVIDENCE that both higher brain centers and afferent feedback control motor behavior through the coordinated activation of specific groups of muscles referred to as synergies (Bernstein 1967; Bizzi et al. 2000, 2002; Cappellini et al. 2006; d'Avella and Bizzi 2005; d'Avella et al. 2003, 2008; Drew et al. 2008; Giszter et al. 2007; Hart and Giszter 2004, 2010; Kargo and Giszter 2008; Krouchev et al. 2006; McCrea 1992; Ting and Macpherson 2005; Tresch et al. 1999, 2002; Tresch and Jarc 2009). According to this concept, the spinal cord contains populations of interneurons that project to, and simultaneously activate, specific populations of motoneurons that in turn actuate the specific groups of muscles (muscle synergies) producing a particular motor action and these interneurons are targets for descending control and proprioceptive regulation. Local inhibitory interactions among these populations may allow descending signals to select an appropriate behavior from the available repertoire (McCrea 1992). Some of these synergies can be nonspecific, i.e., be involved in multiple motor behaviors, and some may contribute to the control of only particular behaviors such as walking (d'Avella and Bizzi 2005). Moreover, such motor synergies may be specific or nonspecific to particular inputs to the spinal circuitry, so that, for example, the spinal central pattern generator (CPG), descending supraspinal inputs, and proprioceptive feedback may engage and use the same, completely different, or overlapping motor synergies. From this point of view, it is interesting to investigate what motoneuronal synergies are engaged by the CPG (in the absence of afferent feedback and cortical control) and whether and how these synergies change with afferent feedback.

Recent studies (Rybak et al. 2006a, 2006b; McCrea and Rybak 2007, 2008) have presented a model in which the spinal locomotor CPG has a two-level organization consisting of a half-center rhythm generator (RG) and pattern formation (PF) circuits. In this organization, the PF circuits mediate the RG control of motoneuronal activity and distribute RG inputs to functionally distinct motoneuronal populations. It has been proposed that PF contains predefined circuits that include populations of interneurons projecting to groups of synergist motoneuronal pools. The motoneuronal pools controlled by a common source at the PF level should display a highly synchronized activity during locomotion and may represent motoneuronal synergies controlled by the CPG. During locomotion, these synergies may be refined by both descending signals from higher centers and peripheral afferent feedback.

The use of fictive locomotion preparations of decerebrate cats offers a unique opportunity to examine patterns of motoneuronal activation and synergies formed by the CPG per se in the absence of afferent feedback and patterned cortical signals. During real locomotion, supraspinal and peripheral afferent inputs may change these activation patterns and synergies to adjust locomotor behavior to changing environment and/or limb mechanics. During this process, the afferent feedback and/or descending supraspinal inputs may operate through the synergies formed by the CPG (i.e., PF) organization, or form and operate through other synergies or use combinations of the above. Revealing these synergies is critically important for understanding the neural control of locomotion and other motor behaviors.

Address for reprint requests and other correspondence: I. A. Rybak, Dept. of Neurobiology and Anatomy, Drexel Univ. College of Medicine, 2900 Queen Lane, Philadelphia, PA 19129 (e-mail: rybak@drexel.edu).

The objectives of this study were *1*) to reconstruct a set of profiles of motoneuronal activity recorded from the major cat hindlimb nerves during fictive locomotion; *2*) to reconstruct the corresponding profiles of muscle activity measured during forward level walking in the cat; *3*) to compare the motoneuronal and muscle profiles and identify possible differences between them that may reflect the specific effects of afferent feedback on the CPG and the activity of different motoneurons; and *4*) to identify the synergist groups of motoneurons operating during fictive locomotion and the muscle synergies engaged during real locomotion and comparatively investigate similarities and differences between these synergies.

Minimum spanning tree (MST)-based clustering methods were used to identify potential synergies operating during both fictive and real locomotion. The results of cluster analysis were further refined by the analysis of time delays between the onsets of activity in potential synergists and by the analysis of the firing behavior of potential synergists during deletions representing various failures in the alternating rhythmic flexor and extensor activities (missing bursts) occurring spontaneously during fictive locomotion (Lafreniere-Roula and McCrea 2005; McCrea and Rybak 2007; Rybak et al. 2006a).

Our results demonstrate a striking similarity between fictive and real locomotion in the activity of several major hindlimb nerves and corresponding muscles, and in the identified synergies. We have also found specific differences in the activity of some motoneuronal pools innervating two-joint muscles and the activity of corresponding muscles. These findings provide important insights into the organization and operation of the spinal locomotor CPG, motor synergies controlled by the CPG, and the afferent control of locomotion.

Some preliminary results of this study have been presented previously in abstract form (Markin et al. 2008).

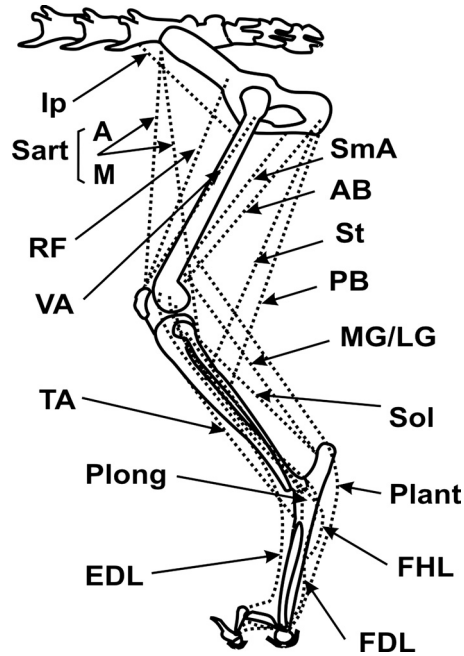


Fig. 1. Schematic representation of major muscles controlling cat hindlimb. AB, anterior biceps; EDL, extensor digitorum longus; FDL, flexor digitorum longus; FHL, flexor hallucis longus; Ip, iliopsoas; LG, lateral gastrocnemius; MG, medial gastrocnemius; PB, posterior biceps; Plant, plantaris; Plong, peroneus longus; RF, rectus femoris; Sart (A and M), sartorius (anterior and medial); SmA, semimembranosus anterior; Sol, soleus; St, semitendinosus; TA, tibialis anterior; VA, vastus. Note that PBSt nerve recorded in fictive locomotion innervates both PB and St muscles and SmAB nerve innervates SmA and AB muscles.

## METHODS

### *Fictive Locomotion Preparation and Electroneurogram Recordings*

All data on the motoneuronal activity during fictive locomotion were taken from the large database of records [electroneurograms (ENGs)] accumulated at the Spinal Cord Research Centre and Department of Physiology, University of Manitoba, by Drs. David McCrea and Larry Jordan during many years of studies on the neural control of locomotion using fictive locomotion cat preparations. These experiments were performed in compliance with the guidelines set out by the Canadian Council for Animal Care and approved by the University of Manitoba Animal Ethics Committee (see Guertin et al. 1995; Lafreniere-Roula and McCrea 2005; Perreault et al. 1999; Stecina et al. 2005; and others). The studies were performed with precollicular-postmammillary decerebrate cats, in which the cortex and all rostral brain stem regions were removed (for details, see Lafreniere-Roula and McCrea 2005). Fictive locomotion was evoked by unilateral or bilateral electrical stimulation of the midbrain locomotor region (MLR) with 0.5-ms-duration current pulses (50–500 mA, 10–20 Hz) after neuromuscular blockade. In each experiment, the ENGs of several (4–9) ipsilateral nerves were simultaneously recorded. Figure 1 provides a schematic representation of the muscles innervated by nerves recorded in these studies. The ENG recordings (98 records from 48 cats, see Table 1) were rectified and digitized at 500 Hz. A representative example of preprocessed raw ENG recordings from one fictive locomotion preparation is shown in Fig. 2*A*. During fictive locomotion, both the total duration of locomotor cycle and the durations of the flexion and extension phases exhibited substantial variability between preparations. Therefore, building a full table of all major motoneuronal activities from many experiments required the development and implementation of special normalization and averaging procedures (see *Data Processing* and APPENDIX).

### *EMG Recordings During Real Locomotion*

Electromyographic activity (EMG) of nine major hindlimb muscles was chronically recorded in six adult female cats (2.5–4.0 kg) during overground and treadmill level walking. All surgical and experimental procedures were in agreement with the *Guide for the Care and Use of Laboratory Animals* (NIH Pub. No. 86-23, 1985) and approved by the Institutional Animal Care and Use Committees of Drexel University and Georgia Institute of Technology.

The methods of animal training, implantations of EMG electrodes, and locomotion data collection have been described elsewhere (Boyce et al. 2007; Gregor et al. 2006; Ollivier-Lanvin et al. 2011; Prilutsky et al. 2011) and are described only briefly here. Prior to surgical implantation of EMG electrodes, cats were trained to walk on a treadmill or across a walkway (3.0 × 0.4 m) with Plexiglas walls with the use of operant conditioning methods and food reward. After completion of training, the skin around the major hindlimb joints was shaved and small reflective markers (6–9 mm in diameter) were attached to bony landmarks with double-sided adhesive tape. Gait of the cat was recorded with a high-speed (120 or 300 Hz) motion capture system (Vicon) during motorized treadmill or overground locomotion, and ground reaction forces were also recorded during overground walking with small (0.16 × 0.11 m) force plates (360 Hz, Bertec) embedded in the floor of the walkway. The kinematics of markers and ground reaction forces were used to identify the timing of stance and swing phases during treadmill and overground locomotion, respectively, to measure speed of overground walking and to confirm that cats demonstrated typical level walking mechanics during EMG data collection.

Table 1. *ENG and EMG data sets*

| Fictive Locomotion | | | | Forward Level Walking | | | |
|---|---|---|---|---|---|---|---|
| Muscle nerves | No. of cats | No. of records | No. of cycles | Muscles | No. of cats | No. of records | No. of cycles |
| Ip | 1 | 4 | 175 | Ip | 5 | 33 | 512 |
| SmAB | 41 | 91 | 2,641 | AB | 5 | 30 | 482 |
| Sart(A or M) | 34 | 77 | 2,059 | SartM | 6 | 44 | 792 |
| PBSt | 29 | 69 | 1,914 | PB | 5 | 28 | 432 |
| RF | 9 | 27 | 652 | RF | 5 | 21 | 363 |
| VA | 8 | 15 | 293 | VA | 6 | 40 | 742 |
| TA | 43 | 92 | 2,662 | TA | 6 | 36 | 665 |
| Plong | 12 | 27 | 876 | | | | |
| EDL | 22 | 39 | 1,305 | | | | |
| MG | 39 | 73 | 2,123 | MG | 6 | 41 | 768 |
| LG/Sol | 17 | 37 | 1,063 | Sol | 6 | 44 | 784 |
| Plant | 14 | 17 | 356 | | | | |
| FHL | 5 | 17 | 733 | | | | |
| FDL | 6 | 10 | 374 | | | | |

ENG, electroneurogram; EMG, electromyogram; AB, anterior biceps; EDL, extensor digitorum longus; FDL, flexor digitorum longus; FHL, flexor hallucis longus; Ip, iliopsoas; LG, lateral gastrocnemius; LG/Sol, lateral gastrocnemius and soleus; MG, medial gastrocnemius; PB, posterior biceps; PBSt, posterior biceps and semitendinosus; Plant, plantaris; Plong, peroneus longus; RF, rectus femoris; Sart (A or M), sartorius (anterior or medial); SmAB, semimembranosus and anterior biceps; Sol, soleus; TA, tibialis anterior; VA, vastus.

After initial locomotion data collection, bipolar EMG electrodes (multistranded, Teflon-insulated, stainless steel wires, AS633 Cooner Wire) were surgically implanted in nine hindlimb muscles unilaterally to record the corresponding EMGs during locomotion (see Figs. 1 and 2*B*): sartorius medialis (SartM, hip flexor, knee flexor), iliopsoas (Ip, hip flexor), anterior biceps femoris (AB, hip extensor), rectus femoris (RF, hip flexor, knee extensor), posterior biceps femoris (PB, hip extensor, knee flexor), vastus medialis or lateralis (VA, knee extensor), tibialis anterior (TA, ankle flexor), soleus (Sol, ankle extensor), and medial or lateral gastrocnemius (MG/LG, ankle extensor, knee flexor). All implanted wires were tunneled subcutaneously to either exit between the two shoulders to attach to a connector mounted on a small jacket worn by the cat or exit at a head-mounted multipin connector. Locations of the EMG electrodes were verified by mild electrical stimulations through the implanted wires.

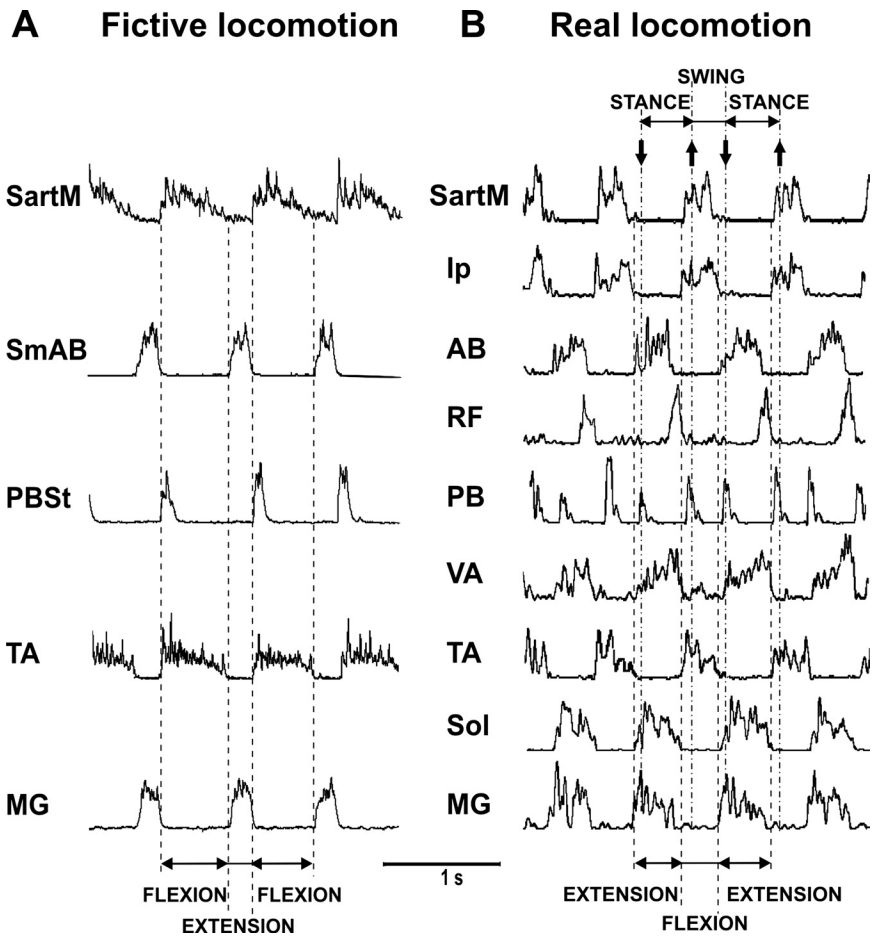


Fig. 2. Representative examples of preprocessed raw recordings from nerves and muscles. *A*: simultaneous recordings of several nerves [electroneurograms (ENGs)] from a fictive locomotion preparation. *B*: simultaneous recording of 9 muscle electromyograms (EMGs) from a cat walking on a treadmill. Both ENGs and EMGs were filtered, rectified, and smoothed (see text). PBSt, PB and St; SmAB, SmA and AB.

After recovery (10–14 days), EMG activity (sampling rate 2,400 Hz, treadmill; 3,000 Hz, overground) and kinematics of walking, as well as ground reaction forces during overground walking, were recorded synchronously as previously described (Boyce et al. 2007; Gregor et al. 2006; Ollivier-Lanvin et al. 2011; Prilutsky et al. 2011; see Table 1). Cats walked overground at a self-selected speed (typically between 0.4 and 0.6 m/s) and on the motorized treadmill at a speed of 0.4 m/s.

The EMG recordings were filtered (band-pass filter 30 Hz to 1 kHz), rectified, and low-pass smoothed by using a binomial smoothing filter with 30 Hz cutoff frequency (Marchand and Marmet 1983). Examples of rectified and smoothed EMG recordings from a freely walking cat are shown in Fig. 2*B*. Since we did not find marked differences in EMG patterns recorded during treadmill and overground locomotion, matching similar observations in cats (Carlson-Kuhta et al. 1998; Smith et al. 1998) and humans (Arsenault et al. 1986; Murray et al. 1985; Nymark et al. 2005), data from both types of experiments were processed together. Records from all experiments were averaged and normalized with the same methods as for the processing of the fictive locomotion data (see below and in APPENDIX).

### *Data Processing*

Only ENG and EMG records that exhibited stable (with <20% variability in both amplitude and burst duration) activity during several consecutive locomotion cycles (not less than 10 for fictive and treadmill locomotion and 4 for overground walking) were chosen for further analysis (Table 1). In each experiment, four to nine different nerves or muscles were recorded simultaneously. Custom software developed at the Spinal Cord Research Centre, University of Manitoba and operating under a Linux operating system was used to detect the timing of burst onset and offset in the preprocessed ENGs recorded during fictive locomotion. The cycle duration in fictive locomotion was defined as the average time between two consecutive flexor or extensor bursts. The burst onset in the ENG of SartM (hip and knee flexor) was considered as the beginning of the flexion phase, and the burst onset in the ENG of semimembranosus-anterior biceps (SmAB, hip extensors) was considered as the beginning of the extension phase (see Figs. 2*A* and 3*A*). Because the locomotion cycle and phase durations varied substantially between preparations, the durations of flexion and extension phases were normalized separately over all experiments (e.g., Berkowitz and Stein 1994; Orlovsky 1972; for details, see APPENDIX). Correspondingly, the timing of onset and offset of ENG bursts in all nerves were represented as portions of the corresponding (flexion or extension) phase, and then motoneuronal activities normalized and averaged within each phase were connected together in the proper sequence.

The locomotion cycle duration for unrestrained walking was defined as the average time between two consecutive moments of liftoff or touchdown that were considered the starting points of the swing and stance phases, respectively. Ground reaction forces were used to evaluate liftoff and touchdown for overground locomotion, while kinematic analyses of the metatarsophalangeal (MTP) and toe markers were used to evaluate liftoff and touchdown for treadmill locomotion. The normalized and averaged EMG profiles for real locomotion were processed with the same methods as for fictive locomotion records (see above).

To compare the averaged ENG and EMG profiles calculated for fictive and unrestrained locomotion, respectively (Figs. 3–5), the normalization coefficients representing the ratios between the average duration of swing and stance phases and the duration of the locomotion cycle during walking were applied to the fictive locomotion profiles to provide the same relative duration for the flexion and extension phases relative to the locomotor cycle. Hence in all cases the locomotion cycle duration was considered to be equal to 1 and the (relative) duration of each phase for fictive locomotion was made equal to that for real locomotion.

### *Cluster Analysis and Determining Motoneuronal and Muscle Synergies*

The cluster analysis applied in this study was based on the approach proposed by Krouchev et al. (2006). Normalized onsets and offsets of all ENG or EMG bursts from all fictive locomotion records and (separately) from all real locomotion records (Table 1) were represented as scatterplots in which the activity burst offset time in a particular ENG/EMG was plotted as a function of its onset time (see Fig. 5, *A* and *B*). Then cluster analysis was used to determine motoneuronal pools or muscle groups that could be considered as functional synergists. Similar to Krouchev et al. (2006), we constructed an adjacency table across nerves or muscles based on the statistical distances between the centers of each cloud of data points that corresponded to the activity of different motoneurons or muscles (see APPENDIX) and used these distances to determine which muscles/motoneuronal pools were active synchronously. However, the value of the $C_{\mathrm{Frac}}$ parameter used by Krouchev et al. to scale distance between the potential clusters did not provide sufficient resolution for our fictive locomotion data sets (specifically, we were unable to cluster both fictive and real locomotion data using the same value of $C_{\mathrm{Frac}}$). Therefore, instead of using the Krouchev et al. method, we utilized the MST clustering algorithm based on graph theory (see Vathy-Fogarassy et al. 2005, 2006; Zahn 1971). This method was used to perform an initial cluster analysis for both fictive and real locomotion data sets. The analysis was performed by representing the data set as an edge-weighted graph $G$ where the vertices represented the full set of nerves or muscles and edges represented statistical distance criteria between pairs of different nerves or muscles. On the basis of a given graph $G$ we found $G_{\mathrm{MST}}$. According to this method, the MST of an edge-weighted graph $G$ (i.e., the $G_{\mathrm{MST}}$) is the spanning tree whose total weight (the sum of the weights of its edges) is not larger than the total weight of any other spanning tree. A subsequent removing of "inconsistent" edges from the $G_{\mathrm{MST}}$ led to a set of subgraphs representing different clusters (see details in APPENDIX).

To verify and refine the results of the initial cluster analysis (which could be affected by the normalization and averaging procedures and not account for other behaviors, such as deletions) we used two additional methods. The first method consisted of testing the statistical difference (*t*-test, significance level 0.05) between the onsets of (ENG or EMG) bursts recorded in the same experiment if they were classified as synergists during the initial cluster analysis, i.e., if they were suggested to belong to the same cluster. This allowed us to correct possible clustering errors resulting from the initial data averaging and normalization.

The second method was used for evaluation and refining of the clustering results for fictive locomotion data sets only. This method was based on the analysis of ENGs of synergists during so-called deletions, which are failures in the alternating rhythmic flexor and extensor activities (missing bursts) occurring spontaneously during fictive locomotion (Lafreniere-Roula and McCrea 2005; McCrea and Rybak 2007; Rybak et al. 2006a). As described previously, deletions usually affect all (or most) motoneurons controlling the same limb, so that during deletions all agonists (e.g., extensors) become silent, whereas all or most antagonists (e.g., flexors) exhibit sustained (or tonic) activity or, sometimes, remain rhythmic (Lafreniere-Roula and McCrea 2005; Rybak et al. 2006a). Therefore, it was suggested that the perturbations producing such deletions occur at the CPG (RG or PF) level and hence should affect all synergists in the same way (McCrea and Rybak 2007; Rybak et al. 2006a). Therefore, the additional criterion applied to fictive locomotion data was that all motoneurons belonging to the same synergy should exhibit similar behavior during deletions.

## RESULTS

### *Analysis of ENG and EMG Profiles During Fictive and Unrestrained Locomotion*

Analyzed data on fictive locomotion included 98 records from 48 cats (with 35 step cycles on average in each record). The fictive locomotion cycle duration in different experiments varied from 400 to 1,800 ms and was 690 ms on average. The averaged and normalized profiles of motoneuronal activities (ENGs) during fictive locomotion are shown in Fig. 3*A*. The activity of all motoneuronal pools for one-joint muscles (both flexor and extensors) fully corresponded to their function, i.e., all flexor nerves were active during the flexion phase and were silent during the extension phase and all extensor nerves were active only during extension. In contrast, the nerves innervating two-joint muscles, such as the posterior biceps and semitendinosus (PBSt, hip extensor and knee flexor) and RF (hip flexor and knee extensor), demonstrated a variety of activity patterns depending on the preparation.

Specifically, PBSt could exhibit one of the following three firing patterns during fictive locomotion (see Fig. 3*A*, *inset*): *1*) a single burst in the beginning of flexion (*type 1* pattern, observed in 73% of cases) that was usually short in duration (<⅓ of the flexion phase) but sometimes longer (up to ⅔ of flexion); *2*) a typical extensor activity, i.e., firing throughout the entire extension phase and being silent during flexion (*type 2* pattern, 9% of cases); or *3*) a biphasic pattern, consisting of a short burst at the very beginning of flexion and a longer activity burst throughout the extension phase (*type 3* pattern, 18% of cases). Similarly, the RF exhibited one of the following two patterns (see Fig. 3*A*, *inset*): *1*) a single burst at the end of flexion (*type 1* pattern, observed in 53% of cases) or *2*) a biphasic pattern consisting of the same burst at the end of flexion and an additional burst at the end of the extension phase (*type 2* pattern, 47%). The exact pattern expressed by the PBSt and RF was dependent on the preparation and remained unchanged during the course of each experiment. Analysis of PBSt and RF activities from experiments in which they were simultaneously recorded revealed the following relations between them (see Fig. 3*A*, *inset*): *1*) when PBSt demonstrated flexor-type activity (i.e., *type 1* pattern), RF exhibited a flexor-type pattern with delayed activity increasing toward the end of flexion (*type 1*) or a biphasic pattern (*type 2*); *2*) when PBSt activity was extensorlike (*type 2*) or biphasic (*type 3*), RF displayed only a flexorlike activity (*type 1*). In other words, if PBSt was active during extension (*type 2* or *3*) then RF did not have an extensor component (i.e., had a *type 1* pattern).

In level treadmill and overground walking studies, we analyzed 46 records from 6 cats; each walked freely overground at a self-selected speed (typically between 0.4 and 0.6 m/s) or on a treadmill at 0.4 m/s. Between five and nine muscles were recorded in each experiment; data were analyzed together. The

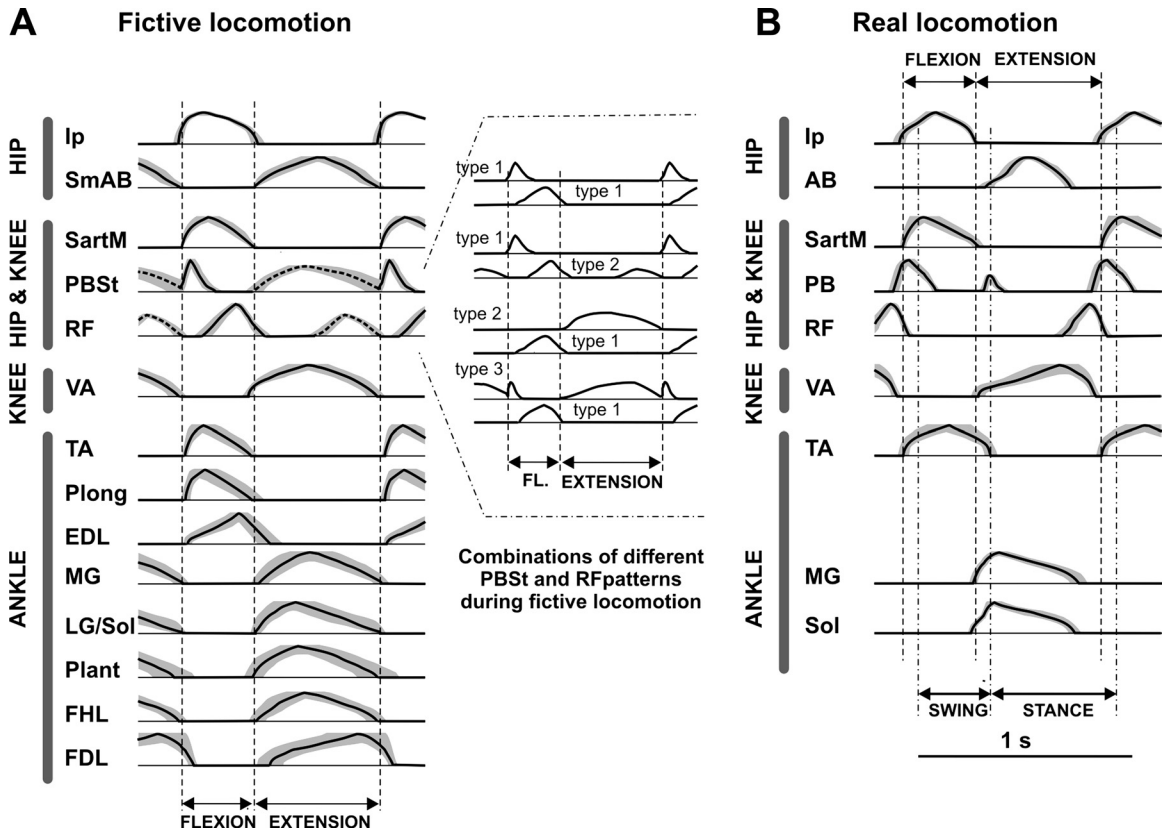


Fig. 3. Hindlimb motoneuronal/muscle activities normalized and averaged over all records during fictive and real level locomotion (see Table 1). The standard deviation (SD) for each pattern is shown as a gray corridor around the corresponding mean trace. Note that according to the normalization and averaging methods used (see APPENDIX), the SD at each point represents deviation in time (but not in amplitude), i.e., ±SD extends left and right. *A*: motoneuronal ENGs normalized and averaged over all experiments during fictive locomotion. Vertical dashed lines indicate onsets of flexion and extension phases. *Inset*: types of PBSt and RF patterns observed during fictive locomotion and their possible combinations (see text for details). *B*: muscle EMGs normalized and averaged over all experiments during unrestrained locomotion. Vertical dash-dotted lines indicate onsets of swing and stance phases; vertical dashed lines show onsets of flexion and extension phases. For abbreviations see Figs. 1 and 2.

locomotion cycle duration in these experiments varied from 800 ms to 1,000 ms and was 920 ms on average. Numbers of consecutive step cycles were between 4 and 62. The durations of swing and stance phases were 330 ± 19.3 ms and 590 ± 51.2 ms, respectively. The averaged profiles of the corresponding muscle EMGs during overground and treadmill locomotion are shown in Fig. 3*B*. These profiles were generally consistent with those recorded in other laboratories and reported in the literature (Engberg and Lundberg 1969; Frigon and Rossignol 2008; Krouchev et al. 2006; Lam and Pearson 2001; Pratt et al. 1991; Rasmussen et al. 1978; Smith et al. 1998).

A qualitative comparison of ENG patterns obtained during fictive locomotion with the corresponding EMG patterns observed in real locomotion (Fig. 4) showed striking similarities in the profiles of one-joint flexors and extensors. However, some differences could be identified. Specifically, the onset of ankle flexors [TA and peroneus longus (Plong), not shown] during fictive locomotion was slightly delayed relative to the onset of hip flexors (Ip and SartM; see Fig. 4), whereas during real locomotion most flexors (Ip, SartM, and TA) were activated almost simultaneously. Also, the TA bursts in real locomotion were longer than during fictive locomotion (Fig. 4). Activity profiles of extensors during both fictive and real locomotion were quite similar. However, VA motoneurons started slightly earlier than motoneurons of other extensors in fictive locomotion, and the bursts of hip and ankle extensors (AB, MG, and Sol) ended earlier in real than in fictive locomotion (Fig. 4).

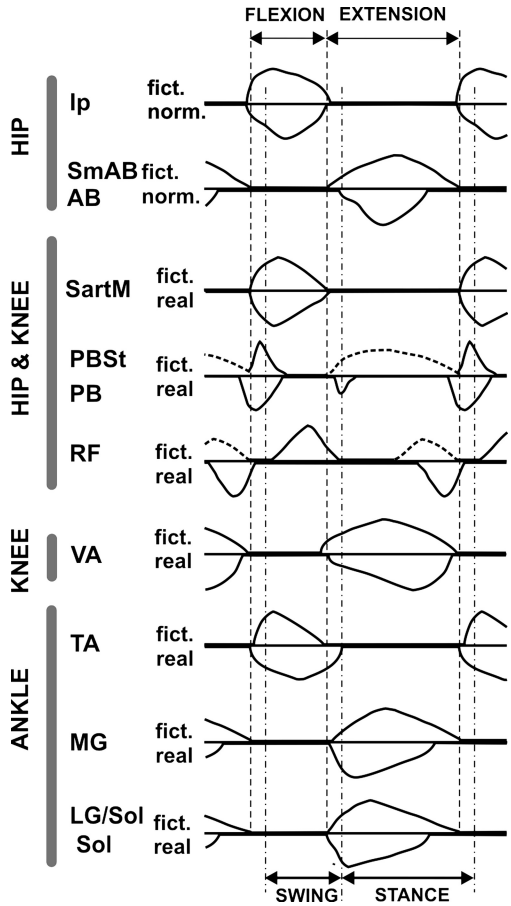


Fig. 4. Comparison of normalized ENG patterns obtained during fictive locomotion with the corresponding normalized EMG patterns recorded during real locomotion. Patterns were taken from Fig. 3, *A* and *B*. The ENG profiles from fictive locomotion (fict.) are shown positive, whereas the EMG profiles from real locomotion (real) are shown negative. For abbreviations see Figs. 1 and 2.

In contrast to the one-joint muscles and the corresponding motoneurons, the activity profiles of proximal nerves innervating two-joint muscles (PBSt and RF) clearly differed from the EMG activity of these muscles recorded during real locomotion (see Fig. 4). Specifically, *1*) the PBSt nerve activity during fictive locomotion never exhibited the short second burst at the end of swing that was recorded from PB in real locomotion; *2*) during real locomotion, the PB did not express a typical extensor activity, which was sometimes present in PBSt nerve during fictive locomotion (PBSt pattern *types 2* and *3* in Fig. 3*A*); and *3*) during real locomotion, the RF never exhibited a flexor burst that could be observed during fictive locomotion, and the onset of its late extensor burst was delayed relative to that in fictive locomotion (Fig. 4).

### *Cluster Analysis*

Cluster analysis was used to identify the nerves and muscles with synergistic activity during fictive (Fig. 5*A*) and real (Fig. 5*B*) locomotion. The same MST-based clustering algorithm was applied to the normalized activity profiles of different nerves or muscles. Activity of 14 nerves was analyzed during fictive locomotion: Ip, SmAB, SartM, PBSt, RF, VA, TA, Plong, extensor digitorum longus (EDL), MG, LG/Sol, plantaris (Plant), flexor hallucis longus (FHL), and flexor digitorum longus (FDL) (see Table 1 and Fig. 5*A*). On the basis of the cluster analysis, all hip and ankle flexor nerves (SartM, Ip, TA, and Plong) were grouped into the same cluster [*cluster (1)* that included *groups 1* and *2*; see Fig. 5*A*]. Also, all hip and ankle extensor nerves (SmAB, MG, LG/Sol, and Plant), FHL, and the extensor burst of PBSt fell into a single cluster [*cluster (3)*, *groups 3a* and *3b*; see Fig. 5*A*]. The VA, flexor bursts of PBSt, RF, EDL, and FDL each represented separate clusters (Fig. 5*A*). Note that when the PBSt was active during extension (pattern *types 2* and *3* in Fig. 3*A*), this extensor activity (Fig. 5*A*) was classified into the cluster containing most of hip and ankle extensors [*cluster (3)*]. In contrast, the PBSt flexor burst (see pattern *types 1* and *3* in Fig. 3*A*) always represented a separate cluster. Also, each RF burst fell into a separate cluster (Fig. 5*A*).

The results of cluster analysis applied to real locomotion are shown in Fig. 5*B*. In contrast to fictive locomotion, the hip flexors (SartM and Ip) and ankle flexor (TA) fell into different clusters [*clusters (1)* and *(2)*, respectively, in Fig. 5*B*]. At the same time, similar to fictive locomotion, all hip and ankle extensors (AB, MG, Sol) belonged to one single cluster (Fig. 5*B*). Also similar to fictive locomotion, VA, PB, and RF each represented a separate cluster. Moreover, each of the two PB bursts represented a separate cluster (Fig. 5*B*).

### *Refining the Results of Cluster Analysis*

*Analysis of absolute delays in burst onset within clusters of potential synergists.* Absolute delays between pairs of ENG or EMG bursts of different nerves or muscles recorded in the same experiment were analyzed. These delays were averaged across trials and experiments. For fictive locomotion, the analysis of delays was applied to ENGs from two clusters that were previously identified by MST method: the cluster of nerves innervating hip and ankle flexors [*cluster (1)* in Fig. 5*A* that included SartM, Ip, TA, and Plong] and the cluster of nerves

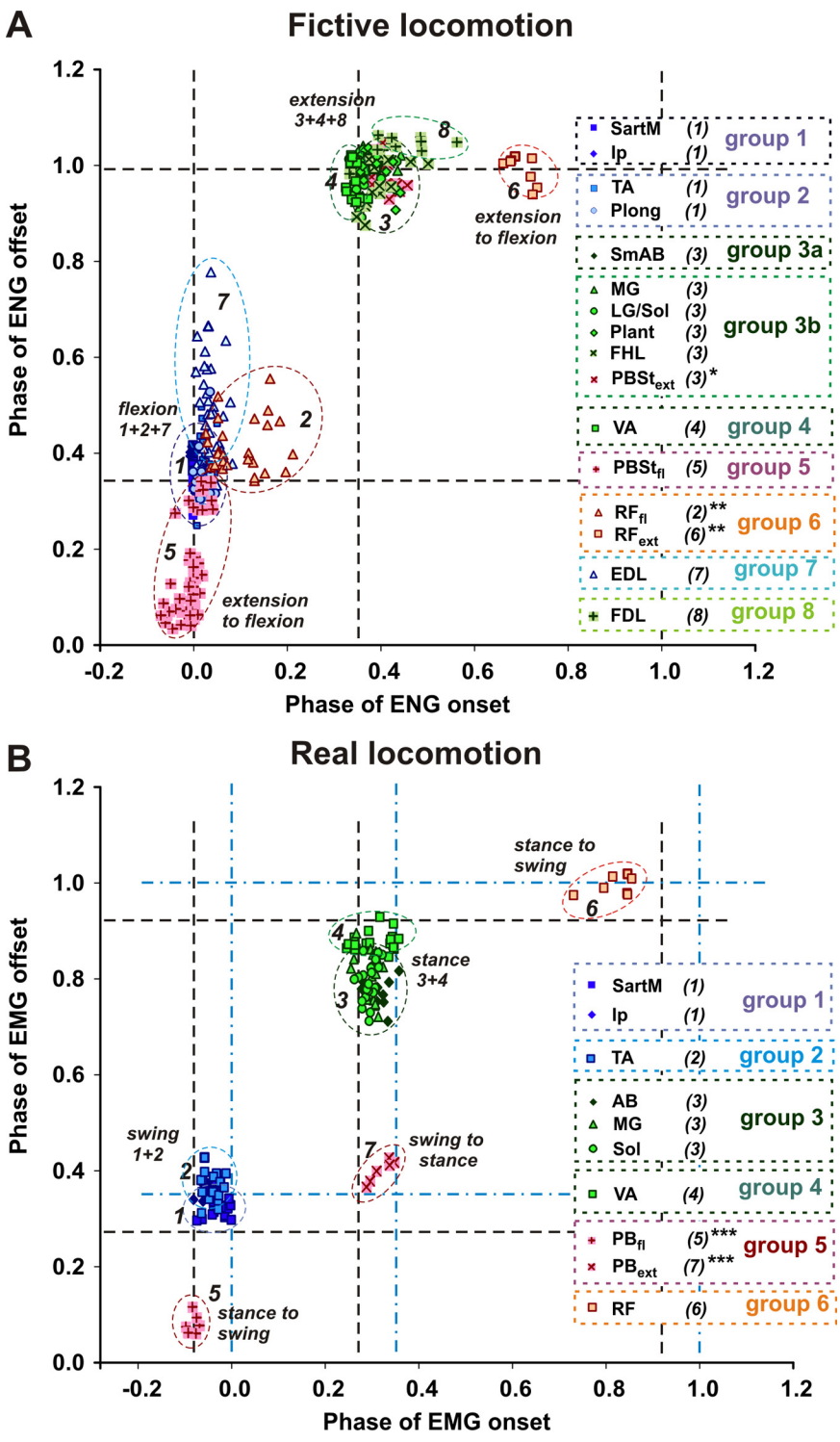


Fig. 5. Scatterplot representation (time of burst offset vs. time of burst onset) of nerve and muscle activity recorded from all cats during fictive and real locomotion, respectively (data shown in Table 1), and the corresponding results of minimum spanning tree (MST) clustering. Each symbol in each plot represents normalized averaged data from 1 analyzed record from Table 1. *A*: scatterplot and MST-based clusters for fictive locomotion. *B*: scatterplot and MST-based clusters for real locomotion. Color ellipses indicate the identified clusters shown on *right*. As a result of normalization, the step cycle period in both plots was equal to 1, with durations of flexion and extension equal to 0.36 and 0.64, respectively. Dashed black lines in both *A* and *B* show onsets of flexion and extension; dash-dotted blue lines in *B* show onsets of swing and stance phases. Identified clusters are numbered in parentheses (*right*). For convenience of data comparison between fictive and real locomotion the same numbering scheme is used for the clusters found in both data sets (*A* and *B*), and 2 identified clusters for fictive locomotion (in *A*) were split into groups [*cluster (1)* into *groups 1* and *2* and *cluster (3)* into *groups 3a* and *3b*]. Note that when the PBSt nerve was active during extension (pattern *types 2* and *3* in Fig. 3*A*), this extensor activity (PBSt$_{ext}$ indicated in *A* by *) was classified into the cluster containing all hip and ankle extensors [*cluster (3)*]. In contrast, the PBSt flexor burst (PBSt$_{fl}$, see pattern *types 1* and *3* in Fig 3*A*) always represented a separate cluster conditionally numbered as *(5)*. Also, each RF burst represents a separate cluster (marked in *A* by **) conditionally numbered as *(2)* and *(7)*. Also, 2 PB EMG bursts in real locomotion (PB$_{fl}$ and PB$_{ext}$ in *B*) initially represented separate *clusters (5)* and *(6)* (marked by ***). For all other clusters identified in fictive and real locomotion, the cluster (and its number) is equal to the corresponding group (and its number). Based on the performed classification, *group 1* of *cluster (1)* in fictive locomotion (*A*) corresponds to *cluster (1)* in real locomotion (*B*); *group 2* of *cluster (1)* in fictive locomotion (*A*) corresponds to *cluster (2)* in real locomotion (*B*); *cluster (3)*, including *groups 3a* and *3b*, in fictive locomotion (*A*) corresponds to *cluster (3)* in real locomotion (*B*); *clusters (4)*, *(5)*, and *(6)* (*groups 4*, *5*, and *6*) in fictive locomotion (*A*) correspond to the corresponding clusters (groups) in real locomotion (*B*). For abbreviations see Figs. 1 and 2. See text for details.

innervating hip and ankle extensors [*cluster (3)* in Fig. 5*A* that included SmAB, MG, LG/Sol, Plant, FHL, and extensor burst of PBSt]. The results of this analysis are shown in Tables 2 and 3, respectively. The analysis showed that the bursts in ankle flexor nerves (TA and Plong) in fictive locomotion started with about a 20-ms delay relative to the onset of hip flexors ($P < 0.05$; see Table 2). At the same time, there were no statistically significant delays between hip flexors or between ankle flexors (Table 2). This allowed us to refine the result of the MST-based clustering analysis and consider hip flexor nerves (SartM and Ip) and ankle flexor nerves as separate synergist groups (*groups 1* and *2* in Fig. 5*A*). Interestingly, this made the clustering results of fictive locomotion more similar to the clustering results of real locomotion, in which hip and ankle flexors also fell into different clusters.

In contrast to the analysis of delays between onsets of flexor nerves, the same analysis of delays between onsets of extensor nerves during fictive locomotion did not show statistically

Table 2. *Delays in ENG burst onset between hip and ankle flexors during fictive locomotion*

| Nerve | SartM | Ip | TA | Plong |
|---|---|---|---|---|
| SartM | x | 8.4 ± 10.81 | 19.7 ± 11.78* | 23.6 ± 12.43* |
| Ip | | x | 26.5 ± 11.92* | n/a |
| TA | | | x | 2.1 ± 11.99 |
| Plong | | | | x |

Values are means ± SD. Numbers within each column (in ms) show the delay in burst onset in the ENG (indicated at the top) relative to the burst onset in the ENG indicated in the left column; n/a indicates that these ENGs were not simultaneously recorded in the same experiment. Numbers of animals, records, and cycles analyzed for each pair of nerves (in parentheses): SartM-Ip (1 cat, 4 records, 159 cycles); SartM-TA (34, 61, 1,844); SartM-Plong (9, 19, 516); Ip-TA (1, 4, 173); TA-Plong, (9, 22, 613). *Statistically significant difference according to *t*-test ($P < 0.05$).

significant delays between the ENG pairs considered (Table 2), which confirmed the results of MST-based classification.

For real locomotion, the analysis of absolute delays was also applied to two clusters identified by the MST method: the cluster of hip flexors [*cluster (1)* in Fig. 5*B* that included SartM and Ip] and the cluster of hip and ankle extensors [*cluster (3)* in Fig. 5*B* that included AB, MG, and Sol]. The results of this analysis for flexors and extensors are shown in Tables 4 and 5, respectively. This analysis did not show statistically significant delays between SartM and Ip (Table 4) and between AB, MG, and Sol (Table 5), hence confirming the results of MST-based classification.

*Analysis of ENG activities during deletions in fictive locomotion.* The objective of this part of the study was to validate and refine the results of cluster analysis by examining the behavior of potential synergists during deletions occurring spontaneously during fictive locomotion. The rationale was based on the idea that the activity of nerves innervating muscles considered synergists (i.e., belonging to the same cluster) should exhibit similar behavior during deletions. In other words, during different deletion types all synergistic ENGs should be silent, switch to sustained (or tonic) activity, or maintain rhythmic activity. We specifically focus on three clusters that were initially classified by MST-based method and refined by the analysis of delays (see above). These clusters included *1*) the cluster of nerves innervating hip flexors (SartM and Ip, *group 1* in Fig. 5*A*), *2*) the cluster of nerves innervating ankle flexors (TA and Plong, *group 2* in Fig. 5*A*), and *3*) the cluster of nerves innervating extensor muscles [SmAB, MG, LG/Sol, Plant, FHL, extensor burst of PBSt if present; *cluster (3)* or *groups 3a* and *3b* together in Fig. 5*A*].

One hundred thirteen deletion episodes during fictive locomotion were analyzed. In all these episodes, if both hip flexor nerves (SartM and Ip) or both ankle flexor nerves (TA and Plong) were recorded in the same experiments, they always demonstrated a consistent behavior, i.e., they were silent during flexor deletions and usually exhibited sustained/tonic activity during extensor deletions. An example is shown in Fig. 6*A*, where during extensor deletion TA, Plong, and SartM switched to a sustained activity. However, the activity of hip flexor and ankle flexor nerves during extensor deletions was not always the same. We found two episodes where during extensor deletion the ankle flexor nerve exhibited sustained activity whereas SartM maintained rhythmic activity (no records of Ip were made in these experiments). An example is shown in Fig. 6*C*. This observation supports the suggestion that ankle and hip flexor nerves belong to different clusters. These observations confirmed our preliminary classification, suggesting that there are two separate flexor clusters, one for hip flexors and the other for ankle flexors.

The behavior of all members of the extensor cluster during deletions (except for SmAB in 2 deletion episodes) was also consistent with the preliminary classification. They all were silent during extensor deletions (MG, LGS, Plant, and SmAB; Fig. 6*A*) and demonstrated sustained/tonic activity during flexor deletions (MG, Plant, and SmAB; Fig. 6*B*). Thus the analysis of deletions generally confirmed our preliminary classification.

At the same time, we found two deletion episodes in which the behavior of SmAB nerve during flexor deletions differed from the behavior of other extensors (see an example in Fig. 6*D*). In these episodes, SmAB nerve was mostly silent during flexor deletion. The existence of such episodes suggests that SmAB should be removed from the common extensor cluster and represented as a separate cluster or group (see *groups 3a* and *3b* in Fig. 5*A*).

## DISCUSSION

### *Muscle Synergies Involved in Control of Unrestrained Locomotion in Cats*

Analysis of potential muscle synergies involved in the control of the cat hindlimb during unrestrained locomotion was previously performed by Krouchev et al. (2006). Our results are consistent with the results of these authors. However, some differences in muscle EMG recordings and clustering results should be noted. Specifically, in the Krouchev et al. study, the

Table 3. *Delays in ENG burst onset between hip and ankle extensors during fictive locomotion*

| Nerve | SmAB | MG | LG/Sol | Plant | FHL | PBSt (ext) |
|---|---|---|---|---|---|---|
| SmAB | x | 8.1 ± 15.44 | −0.9 ± 16.04 | 10.3 ± 23.13 | 13.4 ± 18.6 | 13.2 ± 16.49 |
| MG | | x | −6.7 ± 15.43 | 6.4 ± 27.49 | 10 ± 20.83 | n/a |
| LG/Sol | | | x | 17.55 ± 21.32 | 0.67 ± 14.01 | n/a |
| Plant | | | | x | n/a | n/a |
| FHL | | | | | x | n/a |
| PBSt (ext) | | | | | | x |

Values are means ± SD. Numbers (in ms) within each column show the delay in burst onset in the ENG (indicated at the top) relative to the burst onset in the ENG indicated in the left column; n/a indicates that these motoneurons were not simultaneously recorded in the same experiment. Numbers of animals, records, and cycles analyzed for each pair of nerves (in parentheses): SmAB-MG (36 cats, 68 records, 1,747 cycles); SmAB-LG/Sol (16, 30, 740); SmAB-Plant (13, 15, 280); SmAB-FHL (5, 17, 678); SmAB-PBSt (ext) (8, 16, 486); MG-LG/Sol (13, 24, 586); MG-Plant (10, 11, 181); MG-FHL (3, 13, 464); LG/Sol-Plant (6, 8, 147); LG/Sol-FHL (2, 3, 98). All delays were statistically insignificant (*t*-test, $P > 0.05$).

Table 4. *Delays in EMG burst onset between SartM and Ip during real locomotion*

| Muscle | SartM | Ip |
|---|---|---|
| SartM | x | 7.3 ± 11.08 |
| Ip | | x |

Values are means ± SD. Numbers (in ms) within each column show the delay in burst onset in the EMG (indicated at the top) relative to the burst onset in the EMG indicated in the left column. Numbers of animals, records, and cycles analyzed were 5, 30, and 454, respectively. Delay between the bursts of SartM and Ip was statistically insignificant (*t*-test, $P > 0.05$).

ankle flexor TA started firing a bit earlier than other flexors (e.g., SartM), whereas in our experiments the onset of TA was slightly delayed relative to hip flexors (SartM, Ip). This difference could, however, result from differences in the electrode location between the two studies. Also, we did not record FDL and LG during real locomotion, but the recordings from the corresponding nerves during fictive locomotion did not show a small second burst at the onset of flexion, as seen in the EMG records of Krouchev et al. for these muscles. These bursts could result from afferent feedback, which was absent in the fictive locomotion preparations.

Our analysis of real locomotion data identified six groups of synergists, including groups for hip flexors (SartM and Ip), ankle flexor (TA), other extensors (AB, MG, Sol), and separate groups for VA, PB (with 2 separate bursts that could be considered as separate clusters), and RF (see Fig. 5*B*). Comparison with the groups of synergists determined by Krouchev et al. (2006) shows that our classification is fully consistent with their classification, at least regarding the muscles recorded in both studies. However, we need to note that *1*) we did not record from several (5) muscles that were studied by Krouchev et al. (2006), *2*) we recorded from RF, which was not recorded in their study, and *3*) we recorded EMG of PB, whereas Krouchev et al. recorded EMG of semitendinosus (St); however, these EMGs showed similar patterns: two bursts, one at the transition from extension to flexion, and the other at the transition from flexion to extension.

Consistency between the motor synergies proposed in the two studies (despite quite different methods for normalization, averaging, and classification used) provides additional support for the identified synergies. Future studies are needed to investigate whether the identified synergies change with speed of locomotion and slope of support surface (see discussion below) and to what extent the motion-dependent afferent feedback can affect the identified synergies in these cases.

Table 5. *Delays in EMG burst onset between hip and ankle extensors during real locomotion*

| Muscle | AB | MG | Sol |
|---|---|---|---|
| AB | x | −2.8 ± 37.68 | −13.9 ± 33.26 |
| MG | | x | −2.2 ± 19.74 |
| Sol | | | x |

Values are means ± SD. Numbers (in ms) within each column show the delay in burst onset in the EMG (indicated at the top) relative to the burst onset in the EMG indicated in the left column. Numbers of animals, records, and cycles analyzed for each muscle pair (in parentheses): AB-MG (5 cats, 28 records, 422 cycles); AB-Sol (5, 28, 434); MG-Sol (6, 40, 750). All delays were statistically insignificant (*t*-test, $P > 0.05$).

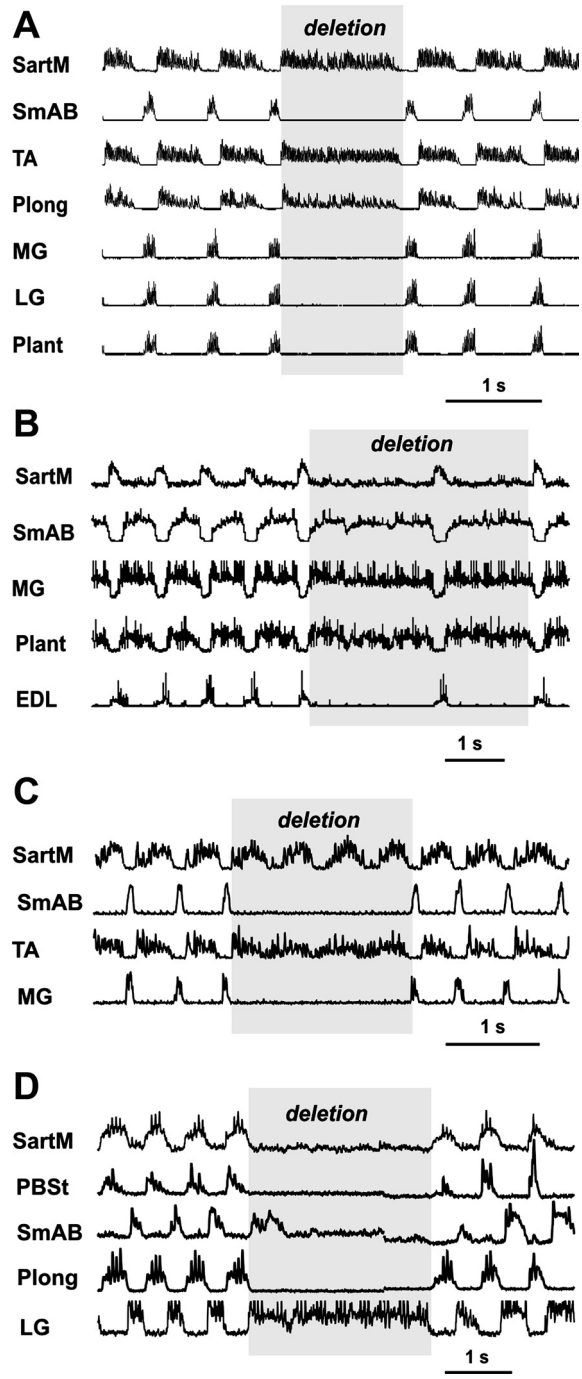


Fig. 6. Examples of typical and atypical deletions during fictive locomotion. *A*: example of typical extensor deletion occurring during midbrain locomotor region (MLR)-evoked fictive locomotion. During this deletion (marked by the gray rectangle), all flexor nerves (SartM, TA, Plong) exhibited sustained activity and all extensor nerves (SmAB, MG, LGS, Plant) were silent. *B*: example of typical flexor deletion during fictive locomotion. During this deletion (marked by the gray rectangle), all extensor nerves (SmAB, MG, Plant) exhibited sustained activity and all flexor nerves (SartM, EDL) were silent. *C*: an atypical extensor deletion, during which ankle flexor nerve TA switched to sustained activity, whereas nerve innervating hip flexor/knee flexor SartM maintained rhythmic activity. *D*: an atypical flexor deletion, in which hip extensor nerve fell silent together with flexor nerves (SartM, PBSt, and Plong). For abbreviations see Figs. 1 and 2.

### *Muscle Synergies Determined from Fictive Locomotion Studies*

Fictive locomotion allowed for identification of the possible synergies used by the locomotor CPG for the control of coordinated motoneuronal activity in the absence of afferent feedback. To our knowledge, this study represents the first attempt to identify such synergies. It should be noted that ENG activity analyzed in the present study was evoked by brain stem (MLR) stimulation and hence may also depend on the organization of brain stem circuits. However, the similarity in fictive locomotor patterns between the decerebrate and spinal cat preparations (see, e.g., Hamm et al. 1999; Nielsen et al. 2005; Pearson and Rossignol 1991) suggests that the ENG patterns and synergies observed in the present study were generated to a large extent by spinal circuits.

Nine groups of synergistic motoneuronal pools controlling hindlimb were identified in this study (Fig. 5*A*), including groups for hip flexors (SartM and Ip) and ankle flexors (TA and Plong), a group for extensors (MG, LG/Sol, Plant, FHL, and extensor activity of PBSt, if present), a separate group for knee extensor VA, a separate group for hip extensor (SmAB, identified based on deletion analysis), and separate groups for EDL, FHL, PBSt (flexor burst), and RF (with 2 separate bursts).

Comparison of this classification with the classification of synergetic muscle activities during real locomotion (from both our study and that of Krouchev et al.) has shown strict similarity in the synergies uncovered, especially for motoneurons controlling one-joint muscles. The major difference occurred in the classification of EDL, FHL, and SmAB, which according to fictive locomotion data each fell in a separate group (Fig. 5*A*).

At the same time, ENG of EDL actually represents a two-joint motoneuronal pool (ankle flexor and digit extensor). Similar to real locomotion, the onset of EDL nerve activity during fictive locomotion coincided with the onset of flexor nerve activity (SartM, Ip, TA, Plong), but the tail of its activity was often prolonged beyond the end of bursts of other flexor nerves and varied from preparation to preparation (see Figs. 3*A* and 5*A*). That probably was the reason why EDL fell into a separate group in our analysis of fictive locomotion data. We believe that during normal level walking the offset in EDL activity is controlled by afferent feedback.

The FDL nerve controls a two-joint FDL muscle (ankle extensor and digit flexor), which is a direct functional antagonist of EDL. Its separation from the common extensor group during fictive locomotion (to which it belongs according to the Krouchev et al. classification) was based on its delayed onset during extension resulting from its antagonism with EDL that expressed a prolonged activity during fictive locomotion (see above). Again, we believe that the onset of FDL activity during real locomotion is controlled by afferent feedback and its interaction with EDL.

The AB recorded in our study during real walking and the biceps femoris (BF) recorded by Krouchev et al. were both included in the common group of extensors (together with MG, LG, Sol, etc.). The SmAB nerve recorded in fictive locomotion usually behaves as a pure extensor (see Figs. 2*A* and 3*A*) and, according to the MST clustering, also belongs to the extensor group (Fig. 5*A*). However, this classification failed to pass the deletion test (see Fig. 6*D*). At the same time, the sometimes inconsistent behavior of SmAB in fictive locomotion during deletions could result from the complex nature of the SmAB nerve, which consists of AB and SmA branches. This issue requires further investigation.

### *Motoneuronal and Muscle Synergies, Locomotor CPG, and Afferent Control of Locomotion*

During locomotion, the activities of most extensor and flexor muscles controlling single joints are locked to the corresponding extensor or flexor phase. However, as seen in the present and many previous studies, muscles spanning more than one joint, such as PB, St, and RF, express more complicated activity patterns (sometimes even exhibiting 2 bursts per walking cycle), which depend on gait, speed, and/or locomotor conditions (Carlson-Kuhta et al. 1998; Halbertsma 1983; Rossignol 1996; Smith et al. 1993, 1998). The complex and nontrivial activity profiles of these muscles and corresponding motoneurons have been considered a strong argument against the bipartite organization of the locomotor CPG proposed by Graham Brown (1914) and expanded by Lundberg, Jankowska, and their colleagues (e.g., Jankowska et al. 1967a, 1967b; Lundberg 1981). Several attempts have been made to resolve this problem within the framework of a bipartite locomotor CPG by suggesting the existence of special intermediate neural networks mediating the control of motoneuronal pools by the bipartite RG (Burke et al. 2001; Orsal et al. 1986; Perret 1983, etc). McCrea, Rybak, and their collaborators (McCrea and Rybak 2007, 2008; Rybak et al. 2006a, 2006b) have recently proposed a two-level CPG organization suggesting that the spinal locomotor CPG contains a bipartite RG and specially organized PF circuitry operating between the RG and motoneurons. According to this concept, PF contains interacting neural populations that are active during a particular phase of the step cycle producing the phase-specific synchronized activation of the corresponding group of synergetic motoneuron pools. A reduced computational model of the two-level CPG model controlling only two antagonist motoneuron pools, flexor and extensor, was developed (Rybak et al. 2006a, 2006b). The model generated a realistic locomotor pattern and reproduced many characteristics of the fictive locomotor pattern including spontaneous non-resetting deletions and various effects of afferent stimulations. However, this reduced model has not explicitly simulated the activity of motoneurons controlling two-joint muscles, such as PBSt and RF, as well as the unique activity profiles of some motoneurons controlling one-joint muscles (e.g., VA). Further development of this model requires knowledge of the organization of synergetic motoneuronal activity, which is necessary for constructing (and suggesting) the neural organization of the PF circuitry allowing the RG (and afferent feedback) to control the specific muscle synergies (predefined genetically or formed during learning or development), including those responsible for generating complex patterns of two-joint muscles, such as PB, St, and RF, and other unique activity profiles, such as that of VA. The results of this work provide necessary insights for the extension of the two-level CPG model (Markin et al. 2011; Shevtsova et al. 2009).

It is necessary to note that the engaged motor synergies may or may not be specific for locomotion. Experiments in frogs suggest that synergies are conserved across a variety of motor behaviors (d'Avella and Bizzi 2005; Hart and Giszter 2004)

and that many complex and automatic movements may be produced by sequential activation of the synergies by sensory feedback or supraspinal commands (d'Avella et al. 2003; Kargo and Giszter 2008). One objective of this study was to compare the profiles of ENG activities recorded during fictive locomotion (in the absence of afferent feedback) with the corresponding profiles of EMGs recorded during level walking; the latter is supposed to be regulated/adjusted by afferent feedback. The other objective was to make comparisons between the potential synergies operating during fictive versus real locomotion and to learn how afferent feedback modifies these synergies. The specific question is whether afferent feedback directly controls the PF, and hence affects motoneurons via the synergies engaged by the CPG, or uses synergies independent of the CPG or even directly controls the activity of individual motoneuronal populations.

An important characteristic of this study was that all comparisons were made after preliminary normalization of all ENG and EMG activities to the corresponding locomotion cycle duration and the corresponding durations of flexion and extension (and swing and stance) phases. We believe that this normalization does not affect our main conclusion about the influence of afferent feedback on the locomotor circuitry. If the activity profiles and groups of synergists identified during fictive and real locomotion remain the same after normalization, then a reasonable suggestion would be that afferent feedback does nothing more than control the durations of the locomotion cycle and flexion/extension phases, i.e., controls only the operation of the RG defining the timing of phase transitions and the durations of locomotor cycle and its phases. On the other hand, any differences in the activity of muscle synergist groups between fictive and real locomotion, independent of the durations of locomotor cycle and locomotor phases, allow for a number of reasonable suggestions about the possible specific and/or direct effects of afferent feedback on the activity of these synergist groups or individual motoneuronal pools.

Let us now consider the differences in the activity profiles between fictive and real locomotion (Figs. 3 and 4). The behaviors of most one-joint flexor and extensor nerves and corresponding muscles during fictive and real locomotion are very similar. In contrast, the behaviors of two-joint muscles and nerves innervating them, such as PB (PBSt), RF, and (with the account of the Krouchev et al. study) EDL and FDL, are different. If we focus for the moment on PB (PBSt) and RF, the comparison of the scatterplot for fictive locomotion (Fig. 5*A*) with the scatterplots for real locomotion (Fig. 5*B* in the present report and Fig. 7 in Krouchev et al. 2006) reveals the following. The contents of major identified groups of potential synergist are very similar if not the same. The location of clouds that correspond to major synergist groups (that are active either throughout flexion or throughout extension) is also similar. Therefore, the activity of these synergist groups is most likely controlled by the CPG and/or by afferent feedback via the CPG (synergies inherent to the CPG organization). Furthermore, the major differences between scatterplots for fictive versus real locomotion include the presence and location of the clouds corresponding to two-joint muscles and motoneurons controlling them. This specifically concerns the muscles/nerves (PB/PBSt and RF) that are usually active for a short time period around the flexion-extension (swing-stance) and/or extension-flexion (stance-swing) transitions. Therefore, the activity of these motoneuronal pools and muscles during real locomotion seems to be mostly dependent on afferent feedback and to a lesser degree on the RG.

Perret and Cabelguen (1980) also reported much more variable patterns of motoneurons innervating two-joint muscles (including PBSt and RF) as opposed to consistent activity of motoneurons controlling one-joint muscles. They explained this difference by the complex nature of connections from a half-center CPG to these motoneurons. A recent study in the isolated neonatal rat spinal cord with an attached hindlimb (Klein et al. 2010) has also found a much greater variability in activity patterns of two-joint RF and St muscles compared with the one-joint hip flexor Ip and the other thigh muscles with actions at both hip and knee joints (adductor magnus and semimembranosus). The multiple patterns of RF and St were preserved after deafferentation, suggesting that both the intrinsic CPG properties and afferent feedback may contribute to their behavior.

### *Activities of Two-Joint Muscles and Mechanical Demands in Different Forms of Locomotion*

The above conclusion about the possible role of motion-dependent feedback in regulating activity of two-joint muscles is consistent with results of previous studies on different forms of real locomotion (see below) in which two-joint muscles of the thigh demonstrated mutable activity patterns whereas one-joint extensors and flexors typically maintained similar reciprocal activity. For example, during cat backward walking, RF and sartorius anterior (hip flexors, knee extensors) are activated prior to stance and maintain activity for most of stance (Buford and Smith 1990; Pratt et al. 1996), a pattern that was not observed in forward level walking or fictive locomotion in our study (Fig. 3) but is consistent with the required hip flexor and knee extensor moments during this task (Perell et al. 1993).

During very slow walking, the typical two-burst pattern of PB (and St) observed in forward level walking (Fig. 3*B*) changes to a one-burst pattern (without the precontact burst; Smith et al. 1993) and becomes similar to *type 1* PBSt fictive locomotion pattern (Fig. 3*A*, *inset*). It may be speculated that during very slow walking, in which the hindlimb angular momentum is insufficient to place the leg in the appropriate position prior to paw contact (Smith et al. 1993), hip flexor and knee extensor activities are required to accomplish this task. This may explain the absence of the St burst and the occasional presence of RF activity during late swing in forward level walking (Engberg and Lundberg 1969; see also the corresponding RF ENG burst in Fig. 3*A*). With increasing locomotion speed from slow walking to fast galloping, the demand for deceleration of the hip flexion and knee extension in late swing is increasing and the late swing St activity grows and reaches the magnitude exceeding the late stance/early swing burst; the latter occasionally disappears at very high galloping speeds (Engberg and Lundberg 1969; Smith et al. 1993).

The activity of two-joint thigh muscles changes markedly during upslope and downslope walking. During upslope walking (27° and 45°), the St and PB pre-paw contact activity becomes a stance-related extensor activity with the burst lasting ~40% (27°) or most of the stance (45°; Figs. 8 and 10 in Carlson-Kuhta et al. 1998). This St and PB activity pattern is

similar to *type 3* PBSt fictive locomotion pattern found in our study (Fig. 3*A*, *inset*). The above changes in St activity during upslope walking compared with level walking can again be explained by the increased demands brought by the simultaneous development of hip extensor and knee flexor moments (Fig. 6 in Gregor et al. 2006).

During downslope walking (−27° and −45°), the demands for hip flexion and knee extension activities in stance increase, as reflected in the magnitudes of hip flexion and knee extension muscle moments (Fig. 6 in Gregor et al. 2006). As expected, the two-joint RF increases its activity substantially during stance in terms of the magnitude and duration and is active throughout the entire stance (Fig. 8 in Smith et al. 1998). We did not observe such ENG patterns of RF in fictive locomotion studies (Fig. 3*A*).

In all above examples, one-joint muscles typically demonstrate simple reciprocal flexion-extension synergies that were observed in both real level walking and fictive locomotion. There is just one exception. During downslope walking, the hip one-joint flexor Ip becomes active during stance with other hindlimb one-joint extensors (VA and Sol), whereas the one-joint hip extensors AB and SmA become silent (Figs. 8, 10 in Smith et al. 1998). This seemingly inconsistent Ip and AB activity corresponds to the task demand to control cat descent using hip flexor activity (Gregor et al. 2006).

It is interesting to note that the activity of two-joint muscles during different tasks in cats and humans including walking, running, jumping, cycling, and isometric exertion of external forces is closely correlated with joint moment demands (for review see Prilutsky 2000). This fact is consistent with the suggestion that the activity of two-joint muscles may be under strong influence of motion-dependent feedback.

The comparison of the normalized ENG patterns recorded during fictive locomotion and the normalized EMG patterns obtained during forward level walking in cats presented in this report is based on the assumption that the MLR stimulation in the decerebrate paralyzed cat evokes locomotor activity patterns that "by default" correspond to level forward walking and can potentially be transformed into activity patterns typical for other types of walking, such as slope forward or backward walking, in the presence of the corresponding motion-dependent afferent feedback and/or additional descending control. This suggestion, however, does not have explicit experimental support so far. We also believe that the asymmetric changes in the phase durations and duty factor (the ratio of stance duration to step cycle duration) with the speed of locomotion (Halbertsma 1983) are provided by afferent feedback regardless of the duty factor of CPG operation (Markin et al. 2010; Spardy et al. 2011a, 2011b), which is currently under debate (Frigon and Gossard 2009; Hayes et al. 2009; Juvin et al. 2007).

### *Concluding Remarks*

The major objective of this study was to gain insight into the role of motion-dependent afferent feedback in the control of locomotor pattern generation by comparing the patterns of locomotor activity during fictive locomotion (with no motion-dependent feedback) with the corresponding pattern of real treadmill and overground locomotion (with feedback). Mean normalized activity patterns of major cat hindlimb muscle nerves (ENG) and muscles (EMG) generated during fictive locomotion of the decerebrate cat and during cat treadmill and overground level locomotion, respectively, were obtained and comparatively analyzed. The ENG and EMG patterns for one-joint muscles were highly similar in terms of their temporal characteristics relative to the locomotor cycle, but not necessarily in terms of exact activity profiles (which were not analyzed in this study). In contrast, the ENG and EMG patterns of two-joint nerves (PBSt, RF) and corresponding muscles (PB, RF) were generally different and the ENG patterns of PBSt and RF during fictive locomotion were highly variable, suggesting that during real walking the two-joint muscles operate under strong control of afferent feedback. The scatterplot representation (Krouchev et al. 2006) and the MST algorithm were used to identify groups of muscles (synergies) that are likely controlled as single groups in both fictive and real locomotion. The obtained results suggest that afferent feedback is involved in the regulation of locomotion via motoneuronal synergies controlled by the CPG but may also directly affect the activity of motoneuronal pools serving two-joint muscles (e.g., PB and RF). Our future studies will focus on the changes in the hindlimb muscle activity profiles and the functional synergies engaged during up- and downslope walking in cats and on the identification and comparative analysis of muscle synergies in spinal cats after locomotor recovery obtained via locomotor training and other methods.

## APPENDIX

### *Normalization and Averaging of ENG and EMG Patterns*

Each ENG/EMG pattern was normalized in both amplitude and phase duration. Normalization was performed separately for the flexion and extension phases and then connected together with a ratio of flexion phase duration to locomotion cycle duration $k = 0.36$, which corresponded to the average ratio of swing phase duration to walking cycle duration from real locomotion data.

Let $\vec{S}^j$ be a $j$th preprocessed particular ENG or EMG recording ($j = 1, 2, \ldots, N$), where $N$ is the total number of records through all experiments. The corresponding normalized pattern $\vec{S}^j_{\text{norm}}$ can be presented as vector $\vec{S}^j_{\text{norm}} = \{(\tau^j_i, a^j_i)\}$, $i = 1, 2, \ldots, M$, where $M$ is the number of the crossing points between original signal $\vec{S}^j$ and amplitude levels $A^j_i$ that are evenly distributed in range $[0, A^j_{\max}]$, where $A^j_{\max}$ is maximal amplitude of the original pattern $\vec{S}^j$ (see Fig. 7*A* for details); $a^j_i$ is the normalized value of the original pattern at the crossing moment $t^j_i$, and $\tau^j_i$ is normalized time $t^j_i$ in regard to the current phase duration ($T^j_{\text{F}}$ or $T^j_{\text{E}}$). The components of normalized vector $\vec{S}^j_{\text{norm}} = \{(\tau^j_i, a^j_i)\}$ were calculated as follows:

$$\tau^j_i = \begin{cases} (1-k)\cdot\dfrac{t^j_i - t^j_{\text{F}}}{T^{j-1}_{\text{E}}}, \text{ if } t^j_i \in \left[t^{j-1}_{\text{E}}, t^j_{\text{F}}\right); \\ k\cdot\dfrac{t^j_i - t^j_{\text{F}}}{T^j_{\text{F}}}, \text{ if } t^j_i \in \left[t^j_{\text{F}}, t^j_{\text{E}}\right); \\ k + (1-k)\cdot\dfrac{t^j_i - t^j_{\text{E}}}{T^j_{\text{E}}}, \text{ if } t^j_i \in \left[t^j_{\text{E}}, t^{j+1}_{\text{F}}\right); \\ 1 + k\cdot\dfrac{t^j_i - t^{j+1}_{\text{F}}}{T^{j+1}_{\text{F}}}, \text{ if } t^j_i \in \left[t^{j+1}_{\text{F}}, t^{j+1}_{\text{E}}\right] \end{cases} \quad (1)$$

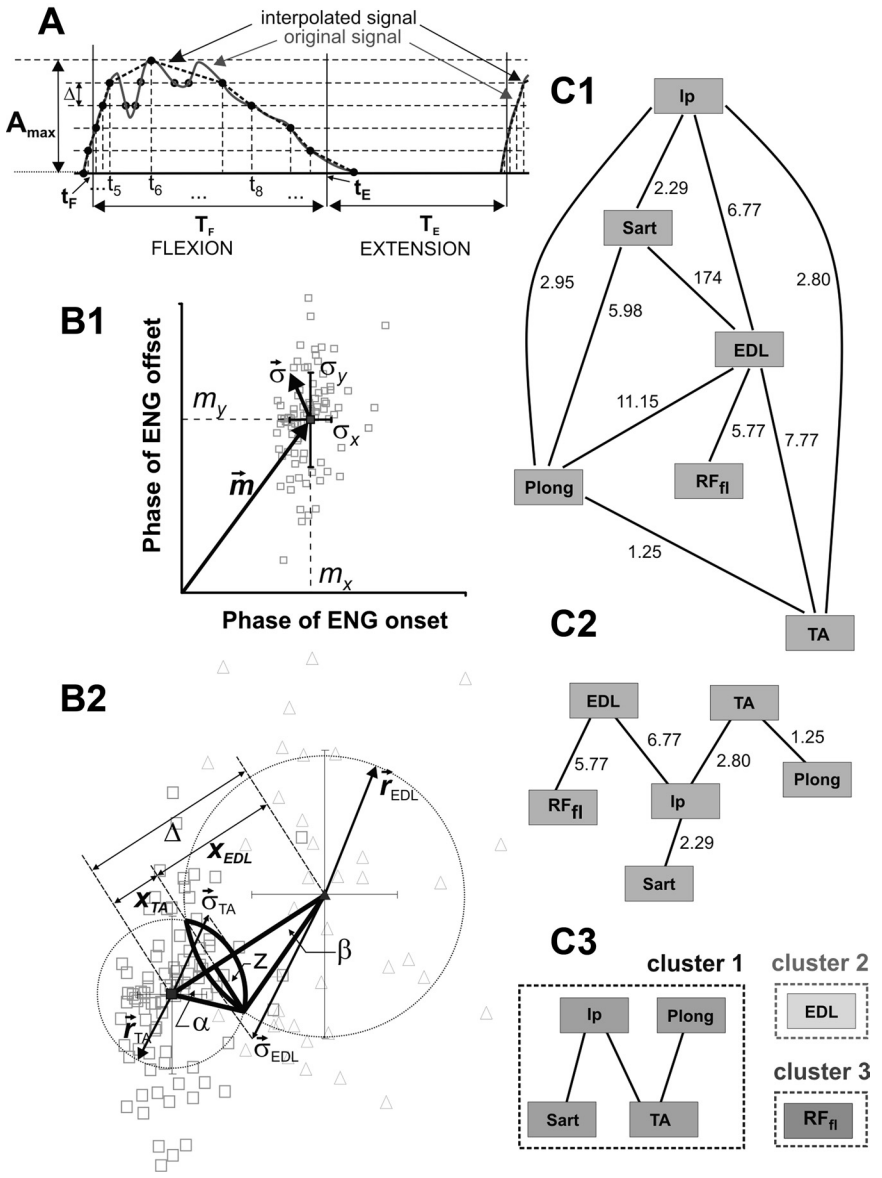


Fig. 7. Normalization, averaging and clusterization of ENG and EMG records. *A*: illustration of normalization method implementation. In this example the recorded activity occurred mostly during flexion. The solid line represents the original preprocessed trace. Interpolated signal $\vec{S}$ (dotted line) is formed by linear interpolation based on 11 points $\{(t_1, A_1), (t_2, A_2), (t_3, A_3), \ldots (t_{11}, A_{11})\}$ that are crossing points (solid small circles) between original signal and 6 amplitude levels ($A_1, A_2 \ldots A_{max}$), where $A_1 = 0$; $A_{i+1} = A_i + \Delta$, $\Delta = A_{max}/5$, $i = 1, 2, \ldots 5$. All internal points for each amplitude level are ignored. To provide sufficient accuracy in the interpolation procedure, 21 amplitude levels were used in the present study. See text for details. *B*: illustration of the clusterization method used in this study. *B1*: representation of 1 cloud in the scatterplot for fictive locomotion. The cloud represents normalized activity of tibialis anterior (TA; gray squares). Vectors $\vec{m}$ and $\vec{\sigma}$ are the mean and standard deviation for all points (gray squares) belonging to the TA cloud. *B2*: calculating the relationships between 2 scatter clouds related to TA (gray squares) and EDL (gray triangles). See text for more details. *C*: illustration of implementation of the MST-based method for cluster analysis of flexor motoneurons during fictive locomotion. *C1*: edge-weighted graph *G* whose vertices represent flexor ENGs recorded in the fictive locomotion experiments and the edges between the vertices represent statistical distance between pairs of ENGs. *C2*: minimal spanning tree $G_{MST}$ derived from graph *G*. *C3*: removal of inconsistent edges from $G_{MST}$ leads to the identification of 3 clusters (see text for details).

$$a_i^j = \frac{A_i^j}{A_{\max}^j}$$

where $t_F^j$ is the onset time of flexion phase and $t_E^j$ is the onset time of extension phase (see Fig. 7*A*).

All normalized patterns were then averaged:

$$\vec{S}_{ENG} = \left\{\left(\bar{\tau}_i, \bar{a}_i\right)\right\} = \begin{cases} \bar{\tau}_i = \dfrac{\sum_j \tau_i^j}{N} \\ \bar{a}_i = \dfrac{\sum_j a_i^j}{N} \end{cases} j = 1, 2, ..N \qquad (2)$$

where $N$ is total number of normalized patterns through all experiments and $\bar{\tau}_i$ and $\bar{a}_i$ are averaged time and amplitude of the averaged pattern $\vec{S}_{ENG}$.

*Cluster Analysis*

Clustering was based on the minimum spanning tree (MST) algorithm available in MATLAB 7.5.0. The MST-based method (e.g., Vathy-Fogarassy et al. 2005, 2006; Zahn 1971) can be briefly described as follows. Let $V = \{v_1, v_2, \ldots v_N\}$ be a set of data with $N$ distinct objects that should be distributed in different groups, where $v_i$ denotes the $i$th object and consists of $n$ measured variables $v_i = \{x_1, x_2, \ldots x_n\}$. Let $e_{ij} = d(v_i, v_j)$ be the distance between any $v_i$ and $v_j$, which can be measured in different ways (e.g., Euclidean distance, Manhattan distance, etc.). Then a set of nodes (vertices) $V = \{v_i\}$ connected by links (edges) $E = \{e_i\}$ can be considered as edges-weighed graph $G = (V, E)$. Removing "inconsistent" edges from the MST of graph $G$ leads to a set of subgraphs that represent different clusters.

Following the method proposed by Krouchev et al. (2006), each normalized ENG or EMG activity was represented as a scatter cloud of points whose Cartesian coordinates represented burst onset and offset, respectively (see Fig. 7*B1*). Vectors $\vec{m}_i = \{m_x^i, m_y^i\}$ and $\vec{\sigma}_i = \{\sigma_x^i, \sigma_y^i\}$ characterize mean and standard deviation for the corresponding scatter cloud of points representing activity of the $i$th nerve or muscle observed in all experiments. A normalized overlapping between two clouds $\omega_{ij}$ can be characterized as follows (see example in Fig. 7*B2*):

$$\omega_{ij} = \begin{cases} \dfrac{\min\left(r_i^2, r_j^2\right)}{\left(r_i^2 + r_j^2\right)/2}, & \left|r_i - r_j\right| \geq \Delta_{ij}; \\ \dfrac{\alpha_{ij} \cdot r_i^2 + \beta_{ij} \cdot r_j^2 - z_{ij} \cdot \left(x_{ij} + x_{ji}\right)}{\pi \cdot \left(r_i^2 + r_j^2\right)/2}, & \left|r_i - r_j\right| < \Delta_{ij} < r_i + r_j; \\ 0, & \Delta_{ij} \geq r_i + r_j \end{cases} \quad (3)$$

where $\Delta_{ij}$ is the distance between the centers of mass of clouds $i$ and $j$; $r_j$ and $r_i$ are the projections of vectors $\vec{\sigma}_i$ and $\vec{\sigma}_j$ onto segment connecting the centers of mass of these clouds:

$$\begin{aligned} x_{ij} &= \left(\Delta_{ij}^2 + r_i^2 - r_j^2\right)/\left(2 \cdot \Delta_{ij}\right); \\ x_{ji} &= \Delta_{ij} - x_{ij}; \\ z_{ij} &= \sqrt{\Delta_{ij}^2 - x_{ij}^2}; \\ \alpha_{ij} &= \arccos\left(x_{ij}/r_i\right); \\ \beta_{ij} &= \arccos\left(x_{ji}/r_j\right) \end{aligned} \quad (4)$$

The "statistical distance" $d_{ij}$ between clouds $i$ and $j$ can be represented as $d_{ij} = \omega_{ij}^{-1}$.

The set of all clouds in the scatterplot can now be considered as an edge-weighted graph $G$ whose vertices represent the full set of nerves or muscles investigated and edges equal to $d_{ij}$ (statistical distance between pairs of different motoneurons or muscles; see an illustration in Fig. 7*C1*).

To determine minimal spanning tree $G_{\mathrm{MST}}$ for the corresponding graph $G$ we used the *graphminspantree* procedure available in MATLAB 7.5.0 (see also Prim 1957). Then any edge $d_{ij}$ between the $i$th and $j$th vertices in $G_{\mathrm{MST}}$ whose value is larger than a selected threshold $\delta$ is considered as "inconsistent" and is removed from the $G_{\mathrm{MST}}$ (Zahn 1971; see an illustration in Fig. 7, *C2* and *C3*). The threshold $\delta$ was calculated as the mean of edges $d_{ij}$ in the $G_{\mathrm{MST}}$ tree. Finally, the vertices that remain connected were considered to belong to the same cluster.

## ACKNOWLEDGMENTS

Authors are greatly thankful to Dr. David A. McCrea for providing direct access to the extensive database of the Spinal Cord Research Centre, University of Manitoba, Winnipeg, MB, Canada, for allowing use of the experimental data on fictive locomotion from this database, and for very useful discussions of the results obtained in this study and earlier drafts of this article.

## GRANTS

This work was supported by the Biomedical Engineering Partnership Program of the National Institutes of Health (NIH) and the National Institute of Neurological Disorders and Stroke (Grant R01 NS-048844) and the National Institute of Biomedical Imaging and Bioengineering (Grant R01 EB-012855). B. I. Prilutsky was also supported by NIH Grant HD-032571 and by the Center for Human Movement Studies, Georgia Tech.

## DISCLOSURES

No conflicts of interest, financial or otherwise, are declared by the author(s). · · ·

## AUTHOR CONTRIBUTIONS

Author contributions: S.N.M. analyzed data; S.N.M., M.A.L., B.I.P., and I.A.R. interpreted results of experiments; S.N.M. and I.A.R. prepared figures; S.N.M., M.A.L., B.I.P., and I.A.R. edited and revised manuscript; S.N.M., M.A.L., B.I.P., and I.A.R. approved final version of manuscript; M.A.L. and B.I.P. performed experiments; I.A.R. conception and design of research; S.N.M. drafted manuscript.

## REFERENCES

**Arsenault AB, Winter DA, Marteniuk RG.** Treadmill versus walkway locomotion in humans: an EMG study. *Ergonomics* 29: 665–676, 1986.

**Berkowitz A, Stein PS.** Activity of descending propriospinal axons in the turtle hindlimb enlargement during two forms of fictive scratching: phase analyses. *J Neurosci* 14: 5105–5119, 1994.

**Bernstein N.** *The Co-ordination and Regulation of Movements*. Oxford, UK: Pergamon, 1967.

**Bizzi E, d'Avella A, Saltiel P, Tresch MC.** Modular organization of spinal motor systems. *Neuroscientist* 8: 437–442, 2002.

**Bizzi E, Tresch MC, Saltiel P, d'Avella A.** New perspectives on spinal motor systems. *Nat Rev Neurosci* 1: 101–108, 2000.

**Boyce VS, Tumolo M, Fischer I, Murray M, Lemay MA.** Neurotrophic factors promote and enhance locomotor recovery in untrained spinalized cats. *J Neurophysiol* 98: 1988–1996, 2007.

**Buford JA, Smith JL.** Adaptive control for backward quadrupedal walking. II. Hindlimb muscle synergies. *J Neurophysiol* 64: 756–766, 1990.

**Burke RE, Degtyarenko AM, Simon ES.** Patterns of locomotor drive to motoneurons and last-order interneurons: clues to the structure of the CPG. *J Neurophysiol* 86: 447–462, 2001.

**Cappellini G, Ivanenko YP, Poppele RE, Lacquaniti F.** Motor patterns in human walking and running. *J Neurophysiol* 95: 3426–3437, 2006.

**Carlson-Kuhta P, Trank TV, Smith JL.** Forms of forward quadrupedal locomotion. II. A comparison of posture, hindlimb kinematics, and motor patterns for upslope and level walking. *J Neurophysiol* 79: 1687–1701, 1998.

**d'Avella A, Bizzi E.** Shared and specific muscle synergies in natural motor behaviors. *Proc Natl Acad Sci USA* 102: 3076–3081, 2005.

**d'Avella A, Fernandez L, Portone A, Lacquaniti F.** Modulation of phasic and tonic muscle synergies with reaching direction and speed. *J Neurophysiol* 100: 1433–1454, 2008.

**d'Avella A, Saltiel P, Bizzi E.** Combinations of muscle synergies in the construction of a natural motor behavior. *Nat Neurosci* 6: 300–308, 2003.

**Drew T, Kalaska J, Krouchev N.** Muscle synergies during locomotion in the cat: a model for motor cortex control. *J Physiol* 586: 1239–1245, 2008.

**Engberg I, Lundberg A.** An electromyographic analysis of muscle activity in the hindlimb of the cat during unrestrained locomotion. *Acta Physiol Scand* 75: 614–630, 1969.

**Frigon A, Gossard JP.** Asymmetric control of cycle period by the spinal locomotor rhythm generator in the adult cat. *J Physiol* 587: 4617–4628, 2009.

**Frigon A, Rossignol S.** Adaptive changes of the locomotor pattern and cutaneous reflexes during locomotion studied in the same cats before and after spinalization. *J Physiol* 586: 2927–2945, 2008.

**Giszter S, Patil V, Hart C.** Primitives, premotor drives, and pattern generation: a combined computational and neuroethological perspective. *Prog Brain Res* 165: 323–346, 2007.

**Graham Brown T.** On the fundamental activity of the nervous centres: together with an analysis of the conditioning of rhythmic activity in progression, and a theory of the evolution of function in the nervous system. *J Physiol* 48: 18–41, 1914.

**Gregor RJ, Smith DW, Prilutsky BI.** Mechanics of slope walking in the cat: quantification of muscle load, length change, and ankle extensor EMG patterns. *J Neurophysiol* 95: 1397–1409, 2006.

**Guertin P, Angel MJ, Perreault MC, McCrea DA.** Ankle extensor group I afferents excite extensors throughout the hindlimb during fictive locomotion in the cat. *J Physiol* 487: 197–209, 1995.

**Halbertsma JM.** The stride cycle of the cat: the modelling of locomotion by computerized analysis of automatic recordings. *Acta Physiol Scand Suppl* 521: 1–75, 1983.

**Hamm TM, Trank TV, Turkin VV.** Correlations between neurograms and locomotor drive potentials in motoneurons during fictive locomotion: implications for the organization of locomotor commands. *Prog Brain Res* 123: 331–339, 1999.

**Hart CB, Giszter SF.** Modular premotor drives and unit bursts as primitives for frog motor behaviors. *J Neurosci* 24: 5269–5282, 2004.

**Hart CB, Giszter SF.** A neural basis for motor primitives in the spinal cord. *J Neurosci* 30: 1322–1336, 2010.

**Hayes HB, Chang YH, Hochman S.** An in vitro spinal cord-hindlimb preparation for studying behaviorally relevant rat locomotor function. *J Neurophysiol* 101: 1114–1122, 2009.

**Jankowska E, Jukes MGM, Lund S, Lundberg A.** The effect of DOPA on the spinal cord. V. Reciprocal organization of pathways transmitting excit-

atory action to alpha motoneurones of flexors and extensors. *Acta Physiol Scand* 70: 369–388, 1967a.

**Jankowska E, Jukes MGM, Lund S, Lundberg A.** The effect of DOPA on the spinal cord. VI. Half-centre organization of interneurones transmitting effects from the flexor reflex afferents. *Acta Physiol Scand* 70: 389–402, 1967b.

**Juvin L, Simmers J, Morin D.** Locomotor rhythmogenesis in the isolated rat spinal cord: a phase-coupled set of symmetrical flexion-extension oscillators. *J Physiol* 583: 115–128, 2007.

**Kargo WJ, Giszter SF.** Individual premotor drive pulses, not time-varying synergies, are the units of adjustment for limb trajectories constructed in spinal cord. *J Neurosci* 28: 2409–2425, 2008.

**Klein DA, Patino A, Tresch MC.** Flexibility of motor pattern generation across stimulation conditions by the neonatal rat spinal cord. *J Neurophysiol* 103: 1580–1590, 2010.

**Krouchev N, Kalaska JF, Drew T.** Sequential activation of muscle synergies during locomotion in the intact cat as revealed by cluster analysis and direct decomposition. *J Neurophysiol* 96: 1991–2010, 2006.

**Lafreniere-Roula M, McCrea DA.** Deletions of rhythmic motoneuron activity during fictive locomotion and scratch provide clues to the organization of the mammalian central pattern generator. *J Neurophysiol* 94: 1120–1132, 2005.

**Lam T, Pearson KG.** Proprioceptive modulation of hip flexor activity during the swing phase of locomotion in decerebrate cats. *J Neurophysiol* 86: 1321–1332, 2001.

**Lundberg A.** Half-centres revisited. In: *Regulatory Functions of the CNS. Motion and Organization Principles*, edited by Szentagothai J, Palkovits M, Hamori J. Budapest: Pergamon Akadem Kiado, 1981, p. 155–167.

**Marchand P, Marmet L.** Binomial smoothing filter: a way to avoid some pitfalls of least square polynomial smoothing. *Rev Sci Instrum* 54: 1034–1041, 1983.

**Markin SN, Klishko AN, Shevtsova NA, Lemay MA, Prilutsky BI, McCrea DA, Rybak IA.** Neuromechanical model of spinal control of locomotion. *Soc Neurosci Abstr* 2011: 919.06, 2011.

**Markin SN, Klishko AN, Shevtsova NA, Lemay MA, Prilutsky BI, Rybak IA.** Afferent control of locomotor CPG: insights from a simple neuromechanical model. *Ann NY Acad Sci* 1198: 21–34, 2010.

**Markin SN, Lemay MA, Ollivier-Lanvin K, Prilutsky BI, McCrea DA, Rybak IA.** Comparison of hindlimb motoneuron activities during fictive and normal locomotion in the cat. *Soc Neurosci Abstr* 2008: 375.13, 2008.

**McCrea DA.** Can sense be made of spinal interneuron circuits? *Behav Brain Sci* 15: 633–643, 1992.

**McCrea DA, Rybak IA.** Modeling the mammalian locomotor CPG: insights from mistakes and perturbations. *Prog Brain Res* 165: 235–253, 2007.

**McCrea DA, Rybak IA.** Organization of mammalian locomotor rhythm and pattern generation. *Brain Res Rev* 57: 134–146, 2008.

**Murray MP, Spurr GB, Sepic SB, Gardner GM, Mollinger LA.** Treadmill vs. floor walking: kinematics, electromyogram, and heart rate. *J Appl Physiol* 59: 87–91, 1985.

**Nielsen JB, Conway BA, Halliday DM, Perreault MC, Hultborn H.** Organization of common synaptic drive to motoneurones during fictive locomotion in the spinal cat. *J Physiol* 569: 291–304, 2005.

**Nymark JR, Balmer SJ, Melis EH, Lemaire ED, Millar S.** Electromyographic and kinematic nondisabled gait differences at extremely slow overground and treadmill walking speeds. *J Rehabil Res Dev* 42: 523–534, 2005.

**Ollivier-Lanvin K, Krupka AJ, AuYong N, Miller K, Prilutsky BI, Lemay MA.** Electrical stimulation of the sural cutaneous afferent nerve controls the amplitude and onset of the swing phase of locomotion in the spinal cat. *J Neurophysiol* 105: 2297–2308, 2011.

**Orlovsky GN.** Activity of vestibulospinal neurons during locomotion. *Brain Res* 46: 85–98, 1972.

**Orsal D, Perret C, Cabelguen JM.** Evidence of rhythmic inhibitory synaptic influences in hindlimb motoneurons during fictive locomotion in the thalamic cat. *Exp Brain Res* 64: 217–224, 1986.

**Pearson KG, Rossignol S.** Fictive motor patterns in chronic spinal cats. *J Neurophysiol* 66: 1874–1887, 1991.

**Perell KL, Gregor RJ, Buford JA, Smith JL.** Adaptive control for backward quadrupedal walking. IV. Hindlimb kinetics during stance and swing. *J Neurophysiol* 70: 2226–2240, 1993.

**Perreault M, Shefchyk SJ, Jimenez I, McCrea DA.** Depression of muscle and cutaneous afferent-evoked monosynaptic field potentials during fictive locomotion in the cat. *J Physiol* 521: 691–703, 1999.

**Perret C.** Centrally generated pattern of motoneuron activity during locomotion in the cat. *Symp Soc Exp Biol* 37: 405–422, 1983.

**Perret C, Cabelguen JM.** Main characteristics of the hindlimb locomotor cycle in the decorticate cat with special reference to bifunctional muscles. *Brain Res* 187: 333–352, 1980.

**Pratt CA, Buford JA, Smith JL.** Adaptive control for backward quadrupedal walking. V. Mutable activation of bifunctional thigh muscles. *J Neurophysiol* 75: 832–842, 1996.

**Pratt CA, Chanaud CM, Loeb GE.** Functionally complex muscles of the cat hindlimb. IV. Intramuscular distribution of movement command signals and cutaneous reflexes in broad, bifunctional thigh muscles. *Exp Brain Res* 85: 281–299, 1991.

**Prilutsky BI.** Coordination of two- and one-joint muscles: functional consequences and implications for motor control. *Motor Control* 4: 1–44, 2000.

**Prilutsky BI, Maas H, Bulgakova M, Hodson-Tole EF, Gregor RJ.** Short-term motor compensations to denervation of feline soleus and lateral gastrocnemius result in preservation of ankle mechanical output during locomotion. *Cells Tissues Organs* 193: 310–324, 2011.

**Prim R.** Shortest connection networks and some generalizations. *Bell Syst Tech J* 36: 1389–1401, 1957.

**Rasmussen S, Chan AK, Goslow GE Jr.** The cat step cycle: electromyographic patterns for hindlimb muscles during posture and unrestrained locomotion. *J Morphol* 155: 253–269, 1978.

**Rossignol S.** Neural control of stereotypic limb movements. In: *Handbook of Physiology. Exercise: Regulation of Integration of Multiple Systems*. Bethesda, MD: Am Physiol Soc, 1996, sect. 12, p. 173–216.

**Rybak IA, Shevtsova NA, Lafreniere-Roula M, McCrea DA.** Modelling spinal circuitry involved in locomotor pattern generation: insights from deletions during fictive locomotion. *J Physiol* 577: 617–639, 2006a.

**Rybak IA, Stecina K, Shevtsova NA, McCrea DA.** Modelling spinal circuitry involved in locomotor pattern generation: insights from the effects of afferent stimulation. *J Physiol* 577: 641–658, 2006b.

**Shevtsova NA, Hamade K, Markin SN, Chakrabarty S, McCrea DA, Rybak IA.** Control of bifunctional motoneurons and locomotor rhythm generation. *Cellular and Network Functions in the Spinal Cord*. Madison, WI, 2009, p. 16.

**Smith JL, Carlson-Kuhta P, Trank TV.** Forms of forward quadrupedal locomotion. III. A comparison of posture, hindlimb kinematics, and motor patterns for downslope and level walking. *J Neurophysiol* 79: 1702–1716, 1998.

**Smith JL, Chung SH, Zernicke RF.** Gait-related motor patterns and hindlimb kinetics for the cat trot and gallop. *Exp Brain Res* 94: 308–322, 1993.

**Spardy LE, Markin SN, Shevtsova NA, Prilutsky BI, Rybak IA, Rubin JE.** A dynamical systems analysis of afferent control in a neuromechanical model of locomotion. I. Rhythm generation. *J Neural Eng* 8: 065003, 2011a.

**Spardy LE, Markin SN, Shevtsova NA, Prilutsky BI, Rybak IA, Rubin JE.** A dynamical systems analysis of afferent control in a neuromechanical model of locomotion. II. Phase asymmetry. *J Neural Eng* 8: 065004, 2011b.

**Stecina K, Quevedo J, McCrea DA.** Parallel reflex pathways from flexor muscle afferents evoking resetting and flexion enhancement during fictive locomotion and scratch in the cat. *J Physiol* 569: 275–290, 2005.

**Ting LH, Macpherson JM.** A limited set of muscle synergies for force control during a postural task. *J Neurophysiol* 93: 609–613, 2005.

**Tresch MC, Jarc A.** The case for and against muscle synergies. *Curr Opin Neurobiol* 19: 601–607, 2009.

**Tresch MC, Saltiel P, Bizzi E.** The construction of movement by the spinal cord. *Nat Neurosci* 2: 162–167, 1999.

**Tresch MC, Saltiel P, d'Avella A, Bizzi E.** Coordination and localization in spinal motor systems. *Brain Res Rev* 40: 66–79, 2002.

**Vathy-Fogarassy A, Feil B, Abonyi J.** Minimal Spanning Tree based fuzzy clustering. *Proc World Acad Sci Eng Tech* 8: 7–12, 2005.

**Vathy-Fogarassy A, Kiss A, Abonyi J.** Hybrid minimal spanning tree and mixture of Gaussians based clustering algorithm. In: *Foundations of Information and Knowledge Systems, Lecture Notes in Computer Science*. Berlin: Springer, 2006, p. 313–330.

**Zahn CT.** Graph-theoretical methods for detecting and describing gestalt clusters. *IEEE Trans Comp* C-20: 68–86, 1971.